Published in final edited form as:
J Neurophysiol. 2002 August ; 88(2): 794–801.

L-Type Calcium Channel-Mediated Plateau Potentials in Barrelette Cells During Structural Plasticity

Fu-Sun Lo and **Reha S. Erzurumlu**
Department of Cell Biology and Anatomy, Louisiana State University Health Sciences Center, New Orleans, Louisiana 70112

Abstract

Development and maintenance of whisker-specific patterns along the rodent trigeminal pathway depends on an intact sensory periphery during the sensitive/critical period in development. Barrelette cells of the brain stem trigeminal nuclei are the first set of neurons to develop whisker-specific patterns. Those in the principal sensory nucleus (PrV) relay these patterns to the ventrobasal thalamus, and consequently, to the somatosensory cortex. Thus PrV barrelette cells are among the first group of central neurons susceptible to the effects of peripheral damage. Previously we showed that membrane properties of barrelette cells are distinct as early as postnatal day 1 (PND 1) and remain unchanged following peripheral denervation in newborn rat pups (Lo and Erzurumlu 2001). In the present study, we investigated the changes in synaptic transmission. In barrelette cells of normal PND 1 rats, weak stimulation of the trigeminal tract (TrV) that was subthreshold for inducing Na^+ spikes evoked an excitatory postsynaptic potential–inhibitory postsynaptic potential (EPSP-IPSP) sequence that was similar to the responses seen in older rats (Lo et al. 1999). Infraorbital nerve transection at birth did not alter excitatory and inhibitory synaptic connections of the barrelette cells. These observations suggested that local neuronal circuits are already established in PrV at birth and remain intact after deafferentation. Strong stimulation of the TrV induced a sustained depolarization (plateau potential) in denervated but not in normal barrelette neurons. The plateau potential was distinct from the EPSP-IPSP sequence by *1*) a sustained (>80 ms) depolarization above −40 mV; *2*) a slow decline slope (<0.1 mV/ms); *3*) partially or totally inactivated Na^+ spikes on the plateau; and *4*) a termination by a steep decay (> 1 mV/ms) to a hyperpolarizing membrane level. The plateau potential was mediated by L-type Ca^{2+} channels and triggered by a *N*-methyl-D-aspartate (NMDA) receptor-mediated EPSP. γ-aminobutyric acid-A ($GABA_A$) receptor-mediated IPSP dynamically regulated the latency and duration of the plateau potential. These results indicate that after neonatal peripheral damage, central trigeminal inputs cause a large and longlasting Ca^{2+} influx through L-type Ca^{2+} channels in barrelette neurons. Increased Ca^{2+} entry may play a key role in injury-induced structural remodeling, and/or transsynaptic cell death.

INTRODUCTION

Afferent terminal arbors and dendritic fields of postsynaptic neurons of the rodent trigeminal pathway develop discrete patterns that replicate the distribution of the whisker and sinus hair follicles on the snout. These patterns are first established in the brain stem trigeminal complex where they are called “barrelettes,” and sequentially in the ventroposteromedial nucleus (VPM) of the dorsal thalamus (“barreloids”) and in layer IV of the primary

Address for reprint requests: F.-S. Lo, Dept. of Cell Biology and Anatomy, LSUHSC, 1901 Perdido St., New Orleans, LA 70112 (flo@lsuhsc.edu).

somatosensory cortex ("barrels") (for reviews, see Erzurumlu and Kind 2001; Killackey et al. 1995; O'Leary et al. 1994; Woolsey 1990). In the rat, barrelette patterns in the brain stem trigeminal nuclei develop before birth (Chiaia et al. 1992) and are dependent on the infraorbital (IO) nerve, which innervates the whiskers and sinus hairs. Trigeminothalamic projection cells (barrelette neurons) of the principal sensory nucleus (PrV) convey this pattern to the VPM, and VPM neurons in turn relay the patterns to the barrel cortex (Erzurumlu and Jhaveri 1990; Erzurumlu and Kind 2001; Killackey and Fleming 1985). Thus along the pathway to neocortex, PrV barrelette neurons are the first set of neurons to detect incoming patterned trigeminal afferents, or any disruption of them.

Previously we showed that barrelette neurons have distinct membrane properties that can be identified between PND 1 and PND 13, and these properties are not altered by IO nerve transection at birth (Lo and Erzurumlu 2001; Lo et al. 1999). This finding was surprising, because following peripheral deafferentation, dramatic changes take place in the PrV: whiskerrelated patterns are lost and a considerable degree of transsynaptic cell death occurs (Bates and Killackey 1985; Miller and Kuhn 1997). In the present study we investigated the development of synaptic transmission in normal PrV, dendritic field alterations in physiologically identified barrelette cells, and their synaptic transmission following denervation. We show that in normal rats, excitatory and inhibitory circuits in the barrelette region of the PrV are established by postnatal day (PND) 1 and IO nerve transection does not change this circuitry. In addition, along with dendritic remodeling, a conspicuous plateau potential emerges in deafferented barrelette neurons. This response is mediated by L-type Ca^{2+} channels. The generation of the plateau depends on activation of *N*-methyl-D-aspartate (NMDA)-type glutamate receptors. γ-Aminobu-tyric acid-A ($GABA_A$) receptor-mediated inhibitory inputs regulate the latency and duration of the plateau potential.

METHODS

Morphological verification of IO nerve transection

We tested dissolution of whisker-specific axon terminal patches in the ventral PrV by biocytin bulk fills. PND 8 Sprague-Dawley rat pups ($n = 6$) which had undergone unilateral IO nerve transection were anesthetized with Fluothane and killed by decapitation. After opening the skull, a cut was made at the midtectal level. Brain tissue rostral to the cut was removed to expose the trigeminal ganglia on both sides. The ganglia were punctured with a hypodermic needle, and biocytin crystals were inserted into the ganglia. Then the brain stem and trigeminal ganglia were dissected out and rinsed thoroughly to wash out biocytin crystals on the surface. Finally the preparation was incubated in artificial cerebrospinal fluid (ACSF) at 33°C for 6–8 h. After fixation in paraformaldehyde for 7 days, the brain stem was sectioned coronally at 500 μm and processed for biocytin reaction. On the normal side, biocytin-reaction product showed clear patches of axon terminals arranged in curvilinear rows reflecting the distribution of whiskers on the snout (Fig. 1*A*). These patterns were similar to those reported with other axonal and histochemical markers (e.g., Bates and Killackey 1985). On the denervated side, axonal patterns were no longer visible (Fig. 1*B*).

We also verified the effects of IO nerve transection by intracellular biocytin labeling. We filled the patch electrodes with 1% biocytin dissolved in potassium-based solution. Once membrane properties and synaptic responses were characterized, the cells were filled intracel-lularly with biocytin by passing AC pulses (±1 nA, 60 ms for each cycle, 100 cycles). One hour after biocytin injection, the slice was immersion fixed in 4% paraformaldehyde in 0.1 M phosphate buffer. The effects of nerve section were reflected in the orientation of dendritic fields of barrelette cells. In the normal PrV, barrelette cells showed polarized dendritic trees ($n = 15$, Fig. 1*C*). As demonstrated previously by others

(Arends and Jacquin 1993), in the denervated PrV, barrelette cells with distinct I_A lost their dendritic orientation, and their dendritic trees became symmetrical ($n = 8$, Fig. 1*D*).

Histological methods

The fixed slice was transferred into phosphate-buffered saline (PBS) at 4°C and then incubated in 10% methanol + 3% H_2O_2 overnight. After several rinses in PBS, the slice was reacted with avidin-biotin complex (ABC Elite kit, Vector Laboratories) overnight at 4°C (1:100 in PBS with 1.8% NaCl and 0.5% Triton X-100). The next day, the slice was rinsed again in PBS and 0.1 M acetate buffer (pH 6.0) and incubated in glucose oxidase–nickel ammonium sulfate and diaminobenzidine until the biocytin labeling could be visualized. The slice was rinsed in acetate buffer and PBS, mounted on a slide, dehydrated, and coverslipped. Labeled cells were drawn with a drawing tube attached to a Nikon Labophot microscope.

Brain slice preparation

PND 0 Sprague-Dawley rat pups were anesthetized with Fluothane and underwent unilateral transection of the IO nerve, and the animals were allowed to survive 4–8 days. They were then overdosed with Fluothane and killed by decapitation. These procedures were approved by the IACUC and followed National Institutes of Health guidelines. The brain was removed and immersed in cold (4°C) sucrose-based ACSF (in mM: 234 sucrose; 2.5 KCl; 1.25 NaH_2PO_4; 10 $MgSO_4$; 24 $NaHCO_3$; 11 glucose; 0.5 $CaCl_2$) bubbled with 95% O_2 −5% CO_2 (pH 7.4). The brain stem was embedded in 2% agar and cut into 400-μm-thick transverse sections with a vibratome (Electron Microscopy Sciences) in the sucrose-based ACSF. Slices containing the PrV were selected, and the normal and denervated side of each slice was marked. After 1 h incubation in normal ACSF (in mM: 124 NaCl; 2.5 KCl; 1.25 NaH_2PO_4; 2 $MgSO_4$; 26 $NaHCO_3$; 10 glucose; 2 $CaCl_2$, pH 7.4) at room temperature, each slice was transferred into a submerged-type recording chamber and continuously perfused (2 ml/ min) with oxygenized normal ACSF at room temperature.

Electrophysiological methods

Whole-cell patch micropipettes were pulled horizontally in two stages from borosilicate glass (WPI, K150F-4) with a P-87 puller (Sutter Instrument Co.). The patch electrodes were backfilled with a potassium-based solution (in mM: 140 K-gluconate; 10 HEPES; 1.1 EGTA-Na; 0.1 $CaCl_2$; 2 $MgCl_2$; 2 ATP-Na; 0.2 GTP-Na, pH 7.25) with a tip resistance of 7–10 MΩ. Neurons in the ventral part of the PrV (barrelette region) were blindly patched with the techniques described by Blanton et al. (1989) and Ferster and Jagadeesh (1992). Patch-electrode resistance was monitored in Bridge Mode of Axoclamp 2B amplifier by measuring the voltage drop induced by a current pulse (−100 pA, 200 ms). An increase in resistance of 20–50 MΩ was taken as a sign that the tip of the electrode contacted the surface of a neuron. A steady negative pressure was applied with a 5-ml syringe to form a gigaohm seal. Then brief suction was used to break into the neuronal soma. The formation of whole-cell configuration was indicated by a sudden drop in seal resistance and a DC drop of >55 mV. After “break-in,” the serial resistance (20–30 MΩ) was completely compensated with bridge balance, and junction potential (Neher 1992) was not corrected. We only collected data from cells with resting membrane potential negative to −55 mV and input resistance >200 MΩ with an Instrutek ITC-16 interface unit and stored on a Pentium III PC with *Pulses* (HEKA) software program.

Different DC pulse protocols were used to induce active conductances of trigeminal neurons. As we reported before (Lo et al. 1999), Barrelette cells in normal PrV were identified by their prominent I_A Following IO nerve transection, barrelette cells still possessed a prominent I_A (Fig. 1, *E* vs. *F*, see also Lo and Erzurumlu 2001) that was

specifically blocked by 1 mM 4-aminopyradine (4-AP, $n = 5$). A pair of fine-tip stimulating electrodes (0.5 MΩ, WPI, IRM33A05KT) was inserted at various points along the trigeminal tract (TrV) lateral to the ventral PrV (barrelette region). Current pulses (0.2- to 0.5-ms duration, 0.05–1.0 mA) were passed through the electrodes at 0.2 Hz to evoke postsynaptic potentials. Identification of excitatory postsynaptic potentials (EPSPs) and inhibitory postsynaptic potentials (IPSPs) was based on their voltage dependency and their responses to glutamate and GABA antagonists. The non-NMDA component of an EPSP increased in amplitude with membrane hyperpolarization. The NMDA component of an EPSP was identified by its nonlinear voltage dependency, slow decay time, and blockade by D-APV (100 μM). The $GABA_A$ receptor-mediated IPSP was identified by its reversal with membrane hyperpolarization (~70 mV) and blockade by bicuculline (10 μM). The synaptically activated L-type Ca^{2+} conductance was blocked by 10 μM nitrendipine. To compare postsynaptic responses among different cells, the membrane potential was held at −60 mV, except in cases where indicated.

RESULTS

If patterning of trigeminal inputs and dendritic orientation of barrelette cells change so dramatically following deafferentation, which aspects of electrophysiological properties of these cells are affected, and how do they relate to structural plasticity or transsynaptic cell death following deafferentation? To address these issues, we examined synaptic responses of deafferented barrelette cells.

Development of postsynaptic responses in barrelette neurons

Trigeminal inputs activate both NMDA and non-NMDA glutamate receptors of the barrelette cells. These cells also receive inhibitory interneuronal inputs mediated by $GABA_A$ receptors (Lo et al. 1999). Postsynaptic potentials in barrelette cells were evoked by stimulation of the TrV at a low intensity (weak stimulus, usually <50 μA) that was subthreshold for inducing postsynaptic spikes. Such stimulation induced an EPSP-IPSP sequence (Fig. 2*A*, *top trace*) as early as PND 1. The IPSPs were reversed in polarity when the membrane potential was hyperpolarized (Fig. 2*A*, *bottom trace*) and blocked by bicuculline (data not shown). This response pattern was also observed in five other cells tested at PND 1, suggesting that neuronal circuitry in PrV is established by birth. At PND 10 or later, the postsynaptic responses of seven barrelette neurons were similar to those at PND 1 (Fig. 2, *A* vs. *B*).

IO nerve transection does not change local neuronal circuitry

In the denervated PrV, stimulation of TrV could still elicit an EPSP-IPSP sequence in barrelette cells (Fig. 2*C*). We recorded synaptic responses from 20 barrelette neurons in denervated PrV at PND 4–8. All of them received excitatory and inhibitory inputs following stimulation of the TrV. Thus IO nerve transection does not alter basic synaptic connections that are normally formed at birth.

IO nerve transection alters synaptic responses to strong stimulation of TrV

In normal barrelette cells, strong stimulation (300–500 μA) of the TrV induced an EPSP with a Na^+ spike riding on it and was followed by a fast decay (>0.5 mV/ms) that resulted from an afterhyperpolarization (AHP) and IPSP (Fig. 3*A*). Stimulation of the TrV with three electrical shocks at 50 Hz evoked three EPSP-spike complexes and a compound hyperpolarization (Fig. 3*D*). In the presence of $GABA_A$ antagonist bicuculline (10 μM), a single shock elicited a long-lasting EPSP with multiple (2–5) spikes (Fig. 3*G*). This was the typical response pattern for most (27/32) barrelette cells in normal PrV. However, in almost all denervated barrelette cells (19/20), single electrical shock resulted in an EPSP-spike

complex that is followed by a sustained depolarization (plateau potential). The plateau potential was distinct from the EPSP-IPSP sequence by *1*) a sustained (>80 ms) depolarization above (positive to) −40 mV; *2*) a slow decline slope (<0.1 mV/ms); *3*) partially or totally inactivated Na^+ spikes on the plateau (Fig. 3*B*); and *4*) then, a steep decay to a hyperpolarizing membrane level (Fig. 4*A*). Since the barrelette cells receive a prominent IPSP (Lo et al. 1999), the plateau potential was sometimes delayed by the IPSP (Fig. 3*C*). Stimulation with three shocks always induced a much longer (>250 ms) plateau potential (Fig. 3, *E* and *F*). Application of bicuculline always prolonged the plateau potential (Fig. 3, *B* vs. *H*; *C* vs. *I*) and shortened the latency of the plateau (Fig. 3*I*).

Voltage- and time-dependence for generation of plateau potential

The mechanism underlying the generation of plateau potentials could be revealed by stimulation of the TrV at different intensities (Fig. 4*A*). A weak stimulus (usually <50 μA) induced an EPSP-IPSP sequence (*trace 1*), while a moderate stimulus (usually <250 μA) evoked a Na^+ spike riding on the EPSP (*trace 2*). A stronger stimulus (around 300 μA) resulted in a plateau potential that started right after the initial Na^+ spike and AHP (*trace 3*). Further increase in stimulation intensity (to 500 μA) caused an increase in amplitude and duration of the plateau potential (*traces 4 and 5*). The threshold of the plateau potential was about −40 mV. Namely, an EPSP that depolarized the membrane above −40 mV would trigger a plateau potential. This voltage-dependency was confirmed by passing hyperpolarizing current. At resting membrane potential (−60 mV), strong stimulation of the TrV could evoke a plateau potential (Fig. 4*B*, *top trace*), whereas at a hyperpolarizing membrane potential (−85 mV), the same stimulus was not able to induce a plateau potential (Fig. 4*B*, *bottom trace*). In addition, the generation of plateau potential depended on the duration of depolarization. The plateau potential was not triggered by the depolarization of the Na^+ spike, because the duration of the spike above −40 mV was very short (<2 ms). As shown in Fig. 4, *A* and *B*, the plateau potential was triggered by the late component of the EPSP, suggesting that its generation is time-dependent. When the EPSP depolarized the membrane above −40 mV for a certain period of time, the plateau potential was induced.

Regulatory effects of inhibitory input on plateau potential

Barrelette cells receive multiple inhibitory inputs (Lo et al. 1999). Because the generation of plateau potential required membrane depolarization caused by excitatory inputs, hyperpolarization from inhibitory inputs (IPSPs) can regulate the plateau potentials. We studied the regulatory effects of inhibition on plateau potentials by application of bicuculline (10 μM, $n = 7$). In the denervated PrV, when the IPSP evoked from stimulation of TrV was of sufficiently large amplitude and long duration, the late component of the EPSP depolarized the membrane below (negative to) −40 mV. Therefore the plateau potential was not induced (Fig. 4*C*, *trace 1*). Bicuculline blocked the IPSP and resulted in a plateau potential (Fig. 4*C*, *trace 2*). This phenomenon was observed in two barrelette cells. Generation of IPSP also delayed the plateau potential. When the IPSP was relatively small, the late component of EPSP could induce a plateau potential after the peak of the IPSP (Fig. 4*D*, *trace 1*). Bicuculline blocked the IPSP and shortened the latency of plateau potential (Fig. 4*D*, *trace 2*). When the IPSP was much smaller in amplitude than the EPSP, strong stimulation induced the plateau potential soon after the onset of IPSP. The IPSP was expressed as a hyperpolarizing notch before the plateau potential (Fig. 4*E*, *trace 1*). Bicuculline abolished the notch and shortened the latency of the plateau (Fig. 4*E*, *trace 2*). Therefore the latency of the plateau varied from 7 to 139 ms ($n = 10$), depending on the algebraic summation of EPSP and IPSP. As soon as the summated potential reached −40 mV, a plateau potential was induced. Bicuculline always shortened the latency of the plateau by 62 ± 6% (mean ± SE, $n = 6$). In addition, generation of IPSP regulated the duration of the plateau potential, because bicuculline prolonged the duration of the plateau (Fig. 4, *D* and *E,*

trace 1 vs. *trace 2*). On average, bicuculline increased the duration of the plateau by 51 ± 12% ($n = 6$).

The plateau potential is mediated by L-type Ca^{2+} channels

The waveform of plateau potential was clearly different from EPSP-IPSP sequence, suggesting some voltage-dependent ion channels were involved in the generation of plateau potential. To test this possibility, we used nitrendipine, an L-type Ca^{2+} channel blocker. Application of nitrendipine (10 μM) completely blocked the plateau potential ($n = 8$) and disclosed the underlying EPSP (Fig. 4*F*, *trace 1* vs. *trace 2*). Before nitrendipine application, the duration of sustained depolarization above −40 mV was 142.9 ± 13.5 ms ($n = 8$). After application of nitrendipine, the duration of depolarization above −40 mV became 12.8 ± 3.1 ms ($n = 8$). The difference in depolarization duration was extremely significant ($P < 0.0001$), indicating that the plateau potential was completely blocked by nitrendipine. This blockade of plateau potential was not caused by a change in synaptic transmission, because at a hyperpolarizing membrane potential (−85 mV), nitrendipine did not affect the size of EPSPs (Fig. 4*G*, *trace 1* vs. *trace 2*).

The plateau potential is triggered by NMDA receptor-mediated EPSP

Since the plateau potential was induced by the late component of the EPSP rather than the Na^+ spike, we bath applied D-APV (100 μM) to block NMDA receptors. D-APV also blocked the plateau potential ($n = 8$) and disclosed the Na^+ spike and non-NMDA component of the EPSP (Fig. 4*H*, *trace 1* vs. *trace 2*). Before application of D-APV, the duration of depolarization above −40 mV was 129.5 ± 11.7 ms ($n = 8$), while after D-APV application, the duration dropped to 6.8 ± 1.3 ms ($n = 8$). This significant change in depolarization duration ($P < 0.0001$) indicated that D-APV completely blocked the plateau potential.

These observations further supported the time-dependency for the generation of the plateau potential. By inference, regenerative activation of L-type Ca^{2+} channels requires >10-ms depolarization above −40 mV, as shown by nitrendipine application. Application of D-APV prevents the plateau potential by shortening the depolarization to < 10 ms. Therefore neither Na^+ spike nor non-NMDA receptor-mediated EPSP can trigger the plateau potential.

DISCUSSION

Following neonatal denervation of the whisker pad, PrV neurons undergo dramatic changes. First, whisker-specific patterning of trigeminal afferent terminals is lost and barrelette cells reorient their dendritic trees from focalized to nonspecific symmetric distribution. These prominent structural changes are easily detected with histochemical stains reflecting synaptic modifications (see Woolsey 1990 for a review). Second, substantial cell death occurs within the denervated PrV through apoptotic mechanisms (Miller and Kuhn 1997). Presently the intracellular signaling pathways and molecular mechanisms underlying structural plasticity of barrelette neurons and apoptotic events are not known. Here we show that, following denervation of the PrV at birth, barrelette neurons display a sustained depolarizing potential (plateau potential) mediated by L-type Ca^{2+} channels. The generation of plateau potential requires activation of NMDA receptors. Furthermore, $GABA_A$ receptor-mediated IPSPs modify the plateau potential in different ways. Presently we do not know to what extent this elevated Ca^{2+} entry into the barrelette cells participates in dendritic remodeling or deafferentation-induced apoptotic events.

Patterned central arbors of single primary afferent fibers in the denervated PrV diffuse after a week following peripheral injury (Bates and Killackey 1985). These changes in afferent organization are accompanied by the rearrangement of barrelette cell dendritic trees as

described in the present study, and previously (Arends and Jacquin 1993). Presumably, during structural modification, single barrelette neurons end up receiving more synaptic inputs than normal PrV. The spatial summation of excitatory inputs results in a compound EPSP that might lead to activation of L-type Ca^{2+} channels. This is supported by the results of a previous study which showed larger and more complex receptive fields in denervated PrV neurons (Waite 1984). The plateau potential most likely results from this increased synaptic activation of barrelette neurons. The L-type Ca^{2+} channel-mediated plateau potential in the denervated PrV is a sustained depolarization with a slow decay, suggesting that it results from regenerative activation of L-type Ca^{2+} channels. Such activation of L-type Ca^{2+} channels requires membrane depolarization above −40 mV for >10 ms; therefore, NMDA receptor-mediated EPSP plays a pivotal role in the generation of plateau potential. In other brain structures, NR2B subunit of the NMDA receptors is gradually replaced by NR2A subunit during postnatal development, so that the duration of NMDA synaptic current is shortened in older animals (see review by Cull-Candy et al. 2001). In the visual cortex, the subunit composition of NMDA receptors is bidirectionally modified by visual experience and deprivation (Philpot et al. 2001; Quinlan et al. 1999a,b). This may also be true for the trigeminal system. In the present study we show that IO nerve transection does not disrupt local neuronal circuits in PrV. However, the subunit composition of NMDA receptors may be changed after IO transection. If denervation delays the replacement of NR2B subunit as shown in the visual cortex, NMDA receptor-mediated EPSP in denervated barrelette cells may have a longer duration than normal ones, that results in a plateau potential. Ongoing studies investigate the possible changes in subunit composition of NMDA receptors after IO transection.

$GABA_A$ receptor-mediated IPSP may delay, shorten, or prevent the generation of the plateau potential. Thus the plateau potential in denervated barrelette neurons may be caused by an absent or diminished $GABA_A$ receptor activity after IO nerve transection. However, this possibility seems unlikely, because our whole-cell recordings from denervated PrV did not reveal a diminished IPSP (see Fig. 2*C*). In addition, application of bicuculline modified the latency or the duration of the plateau potential, suggesting that $GABA_A$-mediated IPSP in denervated PrV is still functional. Another possibility for the induction of plateau potential in denervated PrV is that IO nerve transection increases the expression of L-type Ca^{2+} channels. Immunohistochemical examination of L-type calcium channel expression in normal versus denervated PrV may shed light on this issue.

Synaptically activated plateau potentials have previously been described in a few types of neurons in invertebrates (Dicaprio 1997; Kiehn and Harris-Warrick 1992) and vertebrates (Campbell and Hesslow 1984; Di Prisco et al. 1997; Hounsgaard and Kiehn 1993; Morisset and Nagy 1998; Rekling and Feldman 1997; Russo and Houndgaard 1996). Recently, it was noted that such potentials are prominent during refinement of the rodent visual pathways both in the developing superior colliculus (Lo and Mize 1999, 2000) and in the lateral geniculate nucleus (Lo et al. 2002). Since the rat trigeminal pathway develops much earlier than the visual pathway, we do not know if such potentials are also prominent during the establishment of the barrelettes in late embryonic stages. In most types of neurons, the generation of the plateau potential requires Ca^{2+} influx through L-type Ca^{2+} channel. However, a Ca^{2+}-activated, nonselective cationic conductance (I_{CAN}) may also be involved (Kiehn and Eken 1998; Morisset and Nagy 1999; Pearlstein and Dubuc 1998; Rekling and Feldman 1997; Zhang et al. 1995). The role of L-type Ca^{2+}-mediated plateau potentials in structural and functional plasticity events is not fully understood. In spinal cord dorsal horn neurons, Ca^{2+} influx through L-type channels is a critical component of short-term synaptic plasticity (Morisset and Nagy 2000; Russo and Hounsgaard 1994). In the superior colliculus of neonatal rats, it is associated with the induction of long-term depression of retino-collicular transmission (Lo and Mize 2000). Now, we show that the plateau potential is

present mainly in denervated PrV; it is possible that these potentials play a role in injury-induced plastic rearrangements within the PrV.

Synaptic plasticity and reorganization require an elevation of intracellular concentration of Ca^{2+} through Ca^{2+} release from intracellular stores or Ca^{2+} influx via NMDA receptors or L-type Ca^{2+} channels (Chittajallu et al. 1988; Zuker 1999). Furthermore, activation of NMDA receptors has been shown to play a crucial role in the formation of whisker-specific patterns in the brain (Iwasato et al. 1997, 2000; Li et al. 1994). However, the role of Ca^{2+} influx via L-type channel in pattern formation and injury-induced structural plasticity is still unknown. As judged by membrane potential changes, the Ca^{2+} influx through L-type Ca^{2+} channels is much larger and longer lasting than that through NMDA receptors. L-type Ca^{2+} channels exhibit significantly slower activation kinetics (Fox et al. 1987). Ca^{2+} influx via L-type Ca^{2+} channels could play a particularly important role in signaling pathways for synaptic plasticity, e.g., promoting calmodulin translocation (Deisseroth et al. 1998) and cAMP response element-binding protein (CREB) phosphorylation (Rajadhyaksha et al. 1999), regulating brain-derived neurotrophic factor (BDNF) mRNA expression (Shieh et al. 1998; Tao et al. 1998). A recent study demonstrated that Ca^{2+} influx via L-type channels induces BDNF gene activation more effectively than those evoked via NMDA receptors (Tabuchi et al. 2000). The role of this neurotrophin in dendritic differentiation has been noted (Hirai and Launey 2000; Horch et al. 1999; Mertz et al. 2000). Thus emergence of plateau potentials in denervated barrelette neurons may be linked to their dendritic plasticity.

Synaptic activation of L-type Ca^{2+} channels in denervated PrV could also be associated with the ensuing cell death. During normal development, programmed cell death in the PrV begins at E19 and continues until PND10 (Ashwell and Waite 1991; Miller and Al-Ghoul 1993). Neonatal IO nerve section leads to death of an additional one-third of the PrV neurons through apoptosis (Miller and Kuhn 1997). In light of evidence that several forms of excitotoxicity events are mediated by increased levels of Ca^{2+} influx via L-type Ca^{2+} channels (Freund and Reddig 1994; Leski et al. 1999), the emergence of plateau potentials in denervated barrelette cells could reflect ongoing cell death induced by deafferentation.

Acknowledgments

This research was supported by National Institute of Neurological Disorders and Stroke Grant NS-3707.

REFERENCES

Arends JJ, Jacquin MF. Lucifer Yellow staining in fixed brain slices: optimal methods and compatibility with somatotopic markers in neonatal brain. J Neurosci Methods. 1993; 50:321–339. [PubMed: 8152243]

Ashwell KW, Waite PME. Cell death in the developing trigeminal nuclear complex of the rat. Dev Brain Res. 1991; 63:291–295. [PubMed: 1724212]

Bates CA, Killackey HP. The organization of the neonatal rat's brainstem trigeminal complex and its role in the formation of central patterns. J Comp Neurol. 1985; 240:265–287. [PubMed: 2999198]

Blanton MG, Turco JJL, Kriegstein AR. Whole cell recording from neurons in slices of reptilian and mammalian cerebral cortex. J Neurosci Methods. 1989; 30:203–210. [PubMed: 2607782]

Campbell NC, Hesslow G. Plateau potentials evoked by climbing-fibre stimulation are restricted to the Purkinje cell dendrites of the cat. Neurosci Lett. 1984; 45:187–192. [PubMed: 6328374]

Chiaia NL, Bennett-Clarke CA, Eck M, White FA, Crissman RS, Rhoades RW. Evidence for prenatal competition among the central arbors of trigeminal primary afferent neurons. Neuroscience. 1992; 12:62–76. [PubMed: 1309577]

Chittajallu R, Alford S, Collingridge GL. Ca^{2+} and synaptic plasticity. Cell Calcium. 1988; 24:377–385. [PubMed: 10091007]

Cull-Candy S, Brickley S, Farrant M. NMDA receptor subunits: diversity, development and disease. Curr Opin Neurobiol. 2001; 11:327–335. [PubMed: 11399431]

Deisseroth K, Heist EK, Tsien RW. Translocation of calmodulin to the nucleus supports CREB phosphorylation in hippocampal neurons. Nature. 1998; 392:198–202. [PubMed: 9515967]

Dicaprio R. Plateau potentials in motor neurons in the ventilatory system of the crab. J Exp Biol. 1997; 200:1725–1736. [PubMed: 9319633]

Di Prisco GV, Pearlstein E, Robitaille R, Dubuc R. Role of sensory-evoked NMDA plateau potentials in the initiation of locomotion. Science. 1997; 278:1122–1125. [PubMed: 9353193]

Erzurumlu RS, Jhaveri S. Thalamic axons confer a blueprint of the sensory periphery onto the developing rat somatosensory cortex. Dev Brain Res. 1990; 56:229–234. [PubMed: 2261684]

Erzurumlu RS, Kind PC. Neural activity: sculptor of “barrels” in the neocortex. Trends Neurosci. 2001; 24:589–595. [PubMed: 11576673]

Ferster D, Jagadeesh B. EPSP-IPSP interactions in cat visual cortex studied with in vivo whole-cell patch recording. Neuroscience. 1992; 12:1262–1274. [PubMed: 1556595]

Fox AP, Nowycky MC, Tsien RW. Kinetic and pharmacological properties distinguishing three types of calcium currents in chick sensory neurones. J Physiol (Lond). 1987; 394:149–172. 1987. [PubMed: 2451016]

Freund WD, Reddig S. AMPA/Zn (2+)-induced neurotoxicity in rat primary cortical cultures: involvement of L-type calcium channels. Brain Res. 1994; 22:257–264. [PubMed: 7527288]

Hirai H, Launey T. The regulatory connection between the activity of granule cell NMDA receptors and dendritic differentiation of cerebellar Purkinje cells. Neuroscience. 2000; 15:5217–5224. [PubMed: 10884305]

Horch HW, Kruttgen A, Portbury SD, Katz LC. Destabilization of cortical dendrites and spines by BDNF. Neuron. 1999; 23:353–364. [PubMed: 10399940]

Hounsgaard J, Kiehn O. Calcium spikes and calcium plateaux evoked by differential polarization in dendrites of turtle motoneurones in vitro. J Physiol (Lond). 1993; 468:245–259. [PubMed: 8254508]

Iwasato T, Datwani A, Wolf AM, Nishiyama H, Taguchi Y, Tonegawa S, Knopfel T, Erzurumlu RS, Itohara S. Cortex-restricted disruption of NMDAR1 impairs neuronal patterns in barrel cortex. Nature. 2000; 406:726–731. [PubMed: 10963597]

Iwasato T, Erzurumlu RS, Huerto PT, Sasaoka T, Ulupinar E, Tonegawa S. NMDA receptor-dependent refinement of somatotopic maps. Neuron. 1997; 19:1–20. [PubMed: 9247258]

Kiehn O, Eken T. Functional role of plateau potentials in vertebrate motor neurons. Curr Opin Neurosci. 1998; 8:746–752.

Kiehn O, Harris-Warrick RM. Serotonergic stretch receptors induce plateau properties in a crustacean motor neuron by a dual-conductance mechanism. J Neurophysiol. 1992; 68:485–495. [PubMed: 1527571]

Killackey HP, Bennett-Clarke CA, Rhoades RW. The formation of a cortical somatotopic map. Trends Neurosci. 1995; 18:402–407. [PubMed: 7482806]

Killackey HP, Fleming K. The role of the principal sensory nucleus in central trigeminal pattern formation. Brain Res. 1985; 354:141–145. [PubMed: 4041914]

Leski ML, Valentine SL, Coyle JT. L-type voltage-gated calcium channels modulate kainic acid neurotoxicity in cerebellar granule cells. Brain Res. 1999; 828:27–40. [PubMed: 10320722]

Li Y, Erzurumlu RS, Chen C, Jhaveri S, Tonegawa S. Whisker-related neuronal patterns fail to develop in the brainstem trigeminal nuclei of MDAR1 knockout mice. Cell. 1994; 76:427–437. [PubMed: 8313466]

Lo F-S, Erzurumlu RS. Neonatal deafferentation does not alter membrane properties of trigeminal nucleus principalis neurons. J Neurophysiol. 2001; 85:1088–1098. [PubMed: 11247979]

Lo F-S, Guido W, Erzurumlu RS. Electrophysiological properties and synaptic responses of cells in the trigeminal principal sensory nucleus of postnatal rats. J Neurophysiol. 1999; 82:2765–2775. [PubMed: 10561443]

Lo F-S, Mize RR. Retinal input induces three firing patterns in neurons of the superficial superior colliculus of neonatal rats. J Neurophysiol. 1999; 81:54–958.

Lo F-S, Mize RR. Synaptic regulation of L-type Ca^{2+} channel activity and long-term depression during refinement of the retinocollicular pathway in developing rodent superior colliculus. Neuroscience. 2000; 20 RC58.

Lo F-S, Ziburkus J, Guido W. Synaptically evoked Ca^{2+}-mediated plateau potentials in LGN. J Neurophysiol. 2002; 87:1175–1185. [PubMed: 11877491]

Mertz K, Koscheck T, Schilling K. Brain-derived neurotrophic factor modulates dendritic morphology of cerebellar basket and stellate cells: an in vitro study. Neuroscience. 2000; 97:303–310. [PubMed: 10799762]

Miller MW, Al-Ghoul WM. Numbers of neurons in the developing principal sensory nucleus of the trigeminal nerve: enhanced survival of early-generated neurons over late-generated neurons. J Comp Neurol. 1993; 330:491–501. [PubMed: 8320339]

Miller MW, Kuhn PE. Neonatal transection of the infraorbital nerve increases the expression of proteins related to neuronal death in the principal sensory nucleus of the trigeminal nerve. Brain Res. 1997; 769:233–244. [PubMed: 9374191]

Morisset V, Nagy F. Nociceptive integration in the rat spinal cord: role of nonlinear membrane properties of deep dorsal horn neurons. Eur J Neurosci. 1998; 10:3642–3652. [PubMed: 9875343]

Morisset V, Nagy F. Ionic basis for plateau potentials in deep dorsal horn neurons of rat spinal cord. Neuroscience. 1999; 19:7309–7316. [PubMed: 10460237]

Morisset V, Nagy F. Plateau potential-dependent windup of the response to primary afferent stimuli in rat dorsal horn neurons. Eur J Neurosci. 2000; 12:3087–3095. [PubMed: 10998092]

Neher E. Correction for liquid junction potentials in patch clamp experiments. Methods Enzymol. 1992; 207:123–131. [PubMed: 1528115]

O'Leary DDM, Ruff NL, Dyck RH. Development, critical period plasticity, and adult reorganizations of mammalian somatosensory systems. Curr Opin Neurobiol. 1994; 4:535–544. [PubMed: 7812142]

Pearlstein E, Dubuc R. Cellular mechanisms underlying plateau potentials in lamprey reticulospinal neurons. Soc Neurosci Abstr. 1998; 24:1669.

Philpot BD, Sekhar AK, Shouval HZ, Bear MF. Visual experience and deprivation bidirectionally modify the composition and function of NMDA receptors in visual cortex. Neuron. 2001; 29:157–169. [PubMed: 11182088]

Quinlan EM, Olstein DH, Bear MF. Bidirectional, experience-dependent regulation of *N*-methyl-d-aspartate receptor subunit composition in the rat visual cortex during postnatal development. Proc Natl Acad Sci USA. 1999a; 96:12876–12880. [PubMed: 10536016]

Quinlan EM, Philpot BD, Huganir RL, Bear MF. Rapid, experience-dependent expression of synaptic NMDA receptors in visual cortex in vivo. Nature Neurosci. 1999b; 2:352–357. [PubMed: 10204542]

Rajadhyaksha A, Barczak A, Macias W, Leveque J-C, Lewis LS, Konradi C. L-type Ca^{2+} channels are essential for glutamate-mediated CREB phosphorylation and c-fos gene expression in striatal neurons. Neuroscience. 1999; 19:6348–6359. [PubMed: 10414964]

Rekling JC, Feldman JL. Calcium-dependentplateau potentials in rostral ambiguous neurons in the newborn mouse brain stem in vitro. J Neurophysiol. 1997; 78:2483–2492. [PubMed: 9356399]

Russo RE, Hounsgaard J. Short-term plasticity in turtle dorsal horn neurons mediated by L-type Ca^{2+} channels. Neuroscience. 1994; 61:191–197. [PubMed: 7969900]

Russo RE, Hounsgaard J. Plateau-generating neurons in the dorsal horn in an in vitro preparation of the turtle spinal cord. J Physiol (Lond). 1996; 493:39–54. [PubMed: 8735693]

Shieh PB, Hu S-C, Bobb K, Timmusk T, Ghosh A. Identification of a signaling pathway involved in calcium regulation of BDNF expression. Neuron. 1998; 20:727–740. [PubMed: 9581764]

Tabuchi A, Nakaoka R, Amano K, Yukimine M, Andoh T, Kuraishi Y, Tsuda M. Differential activation of brain-derived neurotrophic factor gene promoters I and III by Ca^{2+} signals evoked via L-type voltage-dependent and *N*-methyl-d-aspartate receptor Ca^{2+} channels. J Biol Chem. 2000; 275:17269–17275. [PubMed: 10748141]

Tao X, Finkbeiner S, Arnold DB, Shaywitz AJ, Greeenberg ME. Ca influx regulates BDNF transcription by a CREB family transcription factor-dependent mechanism. Neuron. 1998; 20:709–726. [PubMed: 9581763]

Waite PME. Rearrangement of neuronal responses in the trigeminal system of the rat following peripheral nerve section. J Physiol (Lond). 1984; 352:425–445. [PubMed: 6747897]

Woolsey, TA. Peripheral alteration and somatosensory system development. In: Coleman, EJ., editor. Development of Sensory Systems in Mammals. New York: Wiley; 1990. p. 461-516.

Zhang B, Wootton JF, Harris-Warrick RM. Calcium-dependent plateau potentials in a crab stomatogastric ganglion motor neuron II. Calcium activated slow inward current. J Neurophysiol. 1995; 74:1938–1946. [PubMed: 8592187]

Zuker RS. Calcium- and activity-dependent synaptic plasticity. Curr Opin. 1999; 9:305–313.

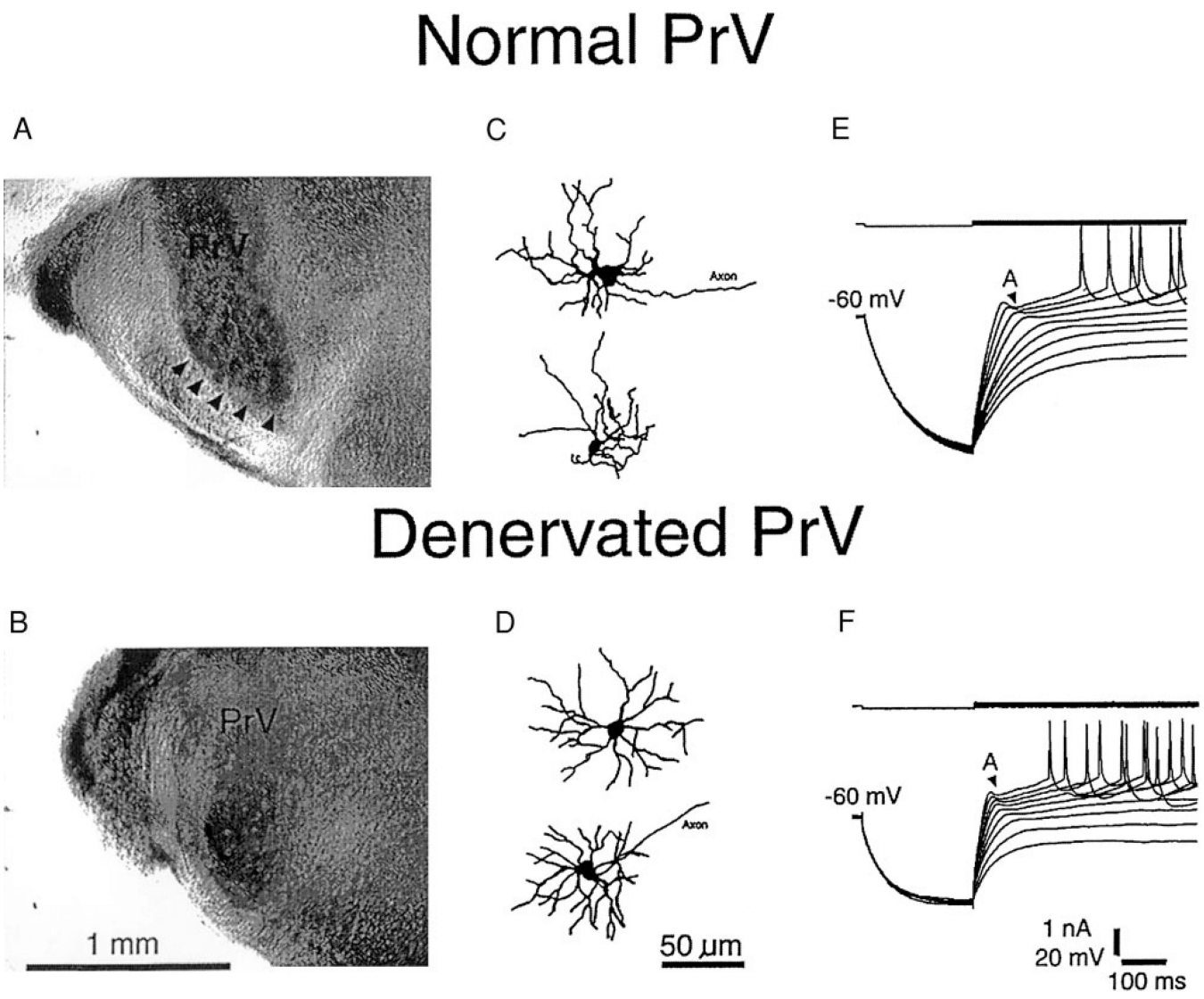

FIG. 1.

Morphological changes in denervated principal sensory nucleus (PrV). *A*: whisker-specific trigeminal afferent arbor patches in normal PrV revealed by ganglionic injection of biocytin. *B*: disappearance of afferent terminal patches in denervated PrV. *C*: examples of biocytin-labeled barrelette cells in normal PrV showing polarized dendritic trees. *D*: examples of biocytin-labeled barrelette cells in denervated PrV showing symmetrical dendritic trees. Both normal (*E*) and denervated (*F*) barrelette cells show a prominent A-type K^+ conductance (I_A) (denoted by A).

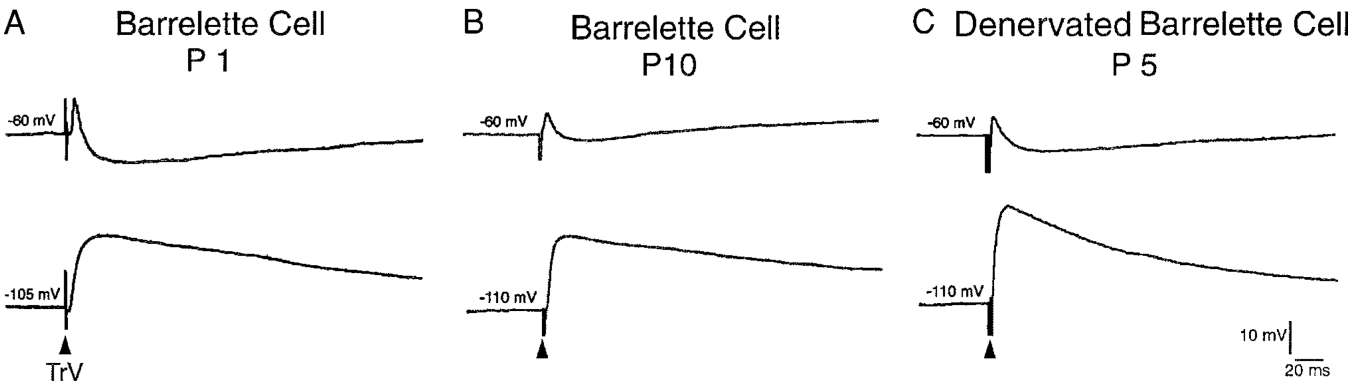

FIG. 2.

Postsynaptic responses to weak stimulation of trigeminal tract (TrV) in barrelette neurons during postnatal development and after infraorbital (IO) nerve transection. *A*: stimulation of TrV at a subthreshold intensity for postsynaptic Na^+ spikes (<50 μA) induced an excitatory postsynaptic potential–inhibitory postsynaptic potential (EPSP-IPSP) sequence in a barrelette cell at PND 1. Note that the IPSP is in hyperpolarizing direction at resting potential (−60 mV). It is reversed into depolarizing direction at −105 mV. *B*: at PND 10, weak stimulation induced an EPSP-IPSP sequence. The IPSP is reversed by membrane hyperpolar-ization (*lower trace*). *C*: weak stimulation of TrV induced an EPSP-IPSP sequence in denervated barrelette cells at PND 5.

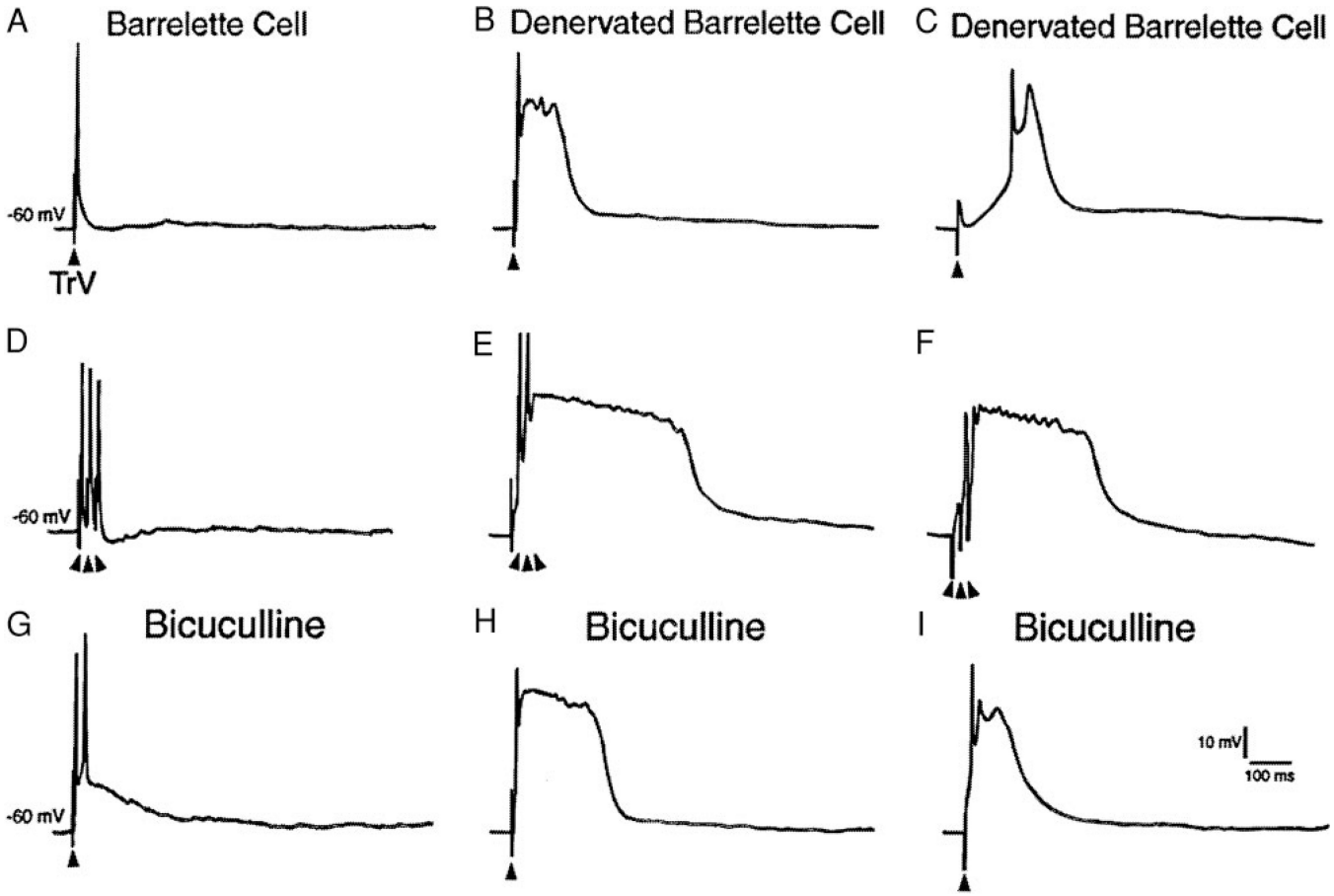

FIG. 3.

Strong stimulation of TrV results in a plateau potential in denervated barrelette cells. *A*: single electrical shock at the maximal intensity (300–500 μA) induces an EPSP-IPSP sequence with a Na^+ spike riding on it in a normal barrelette cell. *B* and *C*: denervated barrelette cells respond to strong stimulation with a plateau potential that appears either immediately after the Na^+ spike (*B*) or after the IPSP (*C*). *D*: in the same normal barrelette cell, 3 shocks at 50 Hz evoked 3 Na^+ spikes riding on 3 EPSP-IPSP sequences. *E* and *F*: in the same denervated barrelette cells, 3 shocks elicited long-lasting plateau potentials. Note that Na^+ spikes are totally or partially inactivated during plateau potentials. *G*: in normal barrelette cell, single shock induces a prolonged EPSP with 2 spikes riding on it in the presence of bicuculline (10 μM) (*E* vs. *A*). *H* and *I*: in the same denervated barrelette cells, application of bicuculline either prolonged the duration of the plateau potential (*H* vs. *B*) or shortened its latency (*I* vs. *C*).

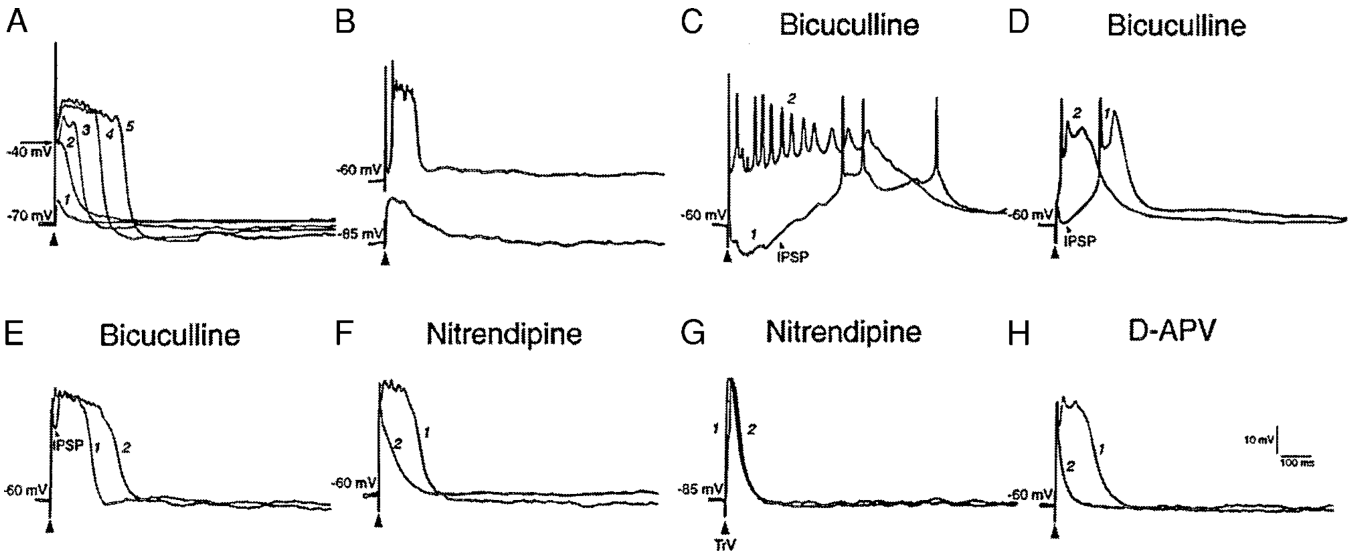

FIG. 4.

Mechanisms underlying the generation of the plateau potential. *A*: stimulation of TrV with increasing intensity increases the EPSP amplitude (*trace 1* vs. *trace 2*) in a denervated barrelette neuron. When the late EPSP reaches above −40 mV, plateau potential is evoked (*trace 3*). Further increase of intensity causes an increase in amplitude and duration of the plateau potential (*traces 4 and 5*). *B*: when the membrane potential is held at −60 mV, strong stimulus results in a plateau potential (*upper trace*). However, at —85 mV, the same stimulus fails to induce a plateau potential (*lower trace*). *C*: single shock at moderate intensity (<250 μA) does not evoke the plateau potential (*trace 1*). In the presence of bicuculline, the same stimulus induces a plateau potential (*trace 2*). *D*: application of bicuculline shortens the latency of plateau potentials (*trace 1*: before; *trace 2*: after drug application). *E*: application of bicuculline prolongs the duration of the plateau potential (*trace 1* vs. *trace 2*). Note that the IPSP is blocked in *trace 2. F*: nitrendipine blocks the plateau potential at −60 mV (*trace 1* vs. *trace 2*). *G*: nitrendipine does not alter the size of the EPSPs in the same cell (*trace 1* vs. *trace 2*). *H*: the plateau potential is blocked by D-APV (100 μM *trace 1* vs. *trace 2*).